



1 GIS-models with fuzzy logic for Susceptibility Maps of debris flow using multiple types of parameters: A Case
2 Study in Pinggu District of Beijing, China
3 Yiwei Zhang¹, Jianping Chen^{1,*}, Qing Wing¹, Chun Tan^{2,3}, Yongchao Li^{4,5,6}, Xiaohui Sun⁷, Yang Li⁸
4
5 1 College of Construction Engineering, Jilin University, Changchun 130026, China
6 2 China Water Northeastern Investigation, Design and Research Co., Ltd, Changchun, Jilin 130026, China
7 3 North China Power Engineering Co., Ltd. of China Power Engineering Consulting Group, Changchun, Jilin
8 130000, China
9 4 Key Laboratory of Shale Gas and Geoengineering, Institute of Geology and Geophysics, Chinese Academy of
10 Sciences, China.
11 5 University of Chinese Academy of Sciences.
12 6 Innovation Academy for Earth Science, Chinese Academy of Sciences, China.
13 7 Department of Earth Sciences and Engineering, Taiyuan University of Technology, Taiyuan 030024, China
14 8 Beijing institute of geological and prospecting engineering, Beijing 100020, China
15 * Corresponding author. Tel.:+86 13843047952
16 * Email address: chenjp@jlu.edu.cn

17
18
19 **Abstract**

20 Debris flow is one of the main causes of life loss and infrastructure damage in mountainous areas, so these
21 hazards must be recognized in the early stage of land development planning. According to field investigation and
22 expert experience, a scientific and effective quantitative susceptibility assessment model was established in Pinggu
23 District of Beijing. This model is based on Geographic Information System (GIS), combining with grey relational
24 method, data-driven and fuzzy logic methods. The inherent influence factors, which are divided into two categories,
25 are selected in the model consistent with the system characteristics of debris flow gully and some new factors are
26 proposed. The results of the 17 models are verified by the results published by the authority, and validated by the
27 other two indexes as well as Area Under Curve (AUC). Through the comparison and analysis of the results, the
28 method to optimize is proposed, including reasonable application of field investigation and expert experience,
29 simplification of factors and scientific classification. Finally, the final optimal susceptibility map with full
30 discussion has the potential to help in determining regional-scale land use planning and debris flow hazard
31 mitigation for decision makers, with full use of insufficient data, scientific calculation, and reliable results. The
32 model has advantages in economically backward areas with insufficient data in mountainous areas.

33 Key words: debris flow; susceptibility assessment; fuzzy logic; model optimization; hazard mitigation
34



35 **1 Introduction**

36 Debris flows are processes of rapid transport of water and soil materials in mountain watersheds, with sudden
37 and destructive outbreaks(Di et al. 2019). Some debris flows can often cause devastating disasters and huge
38 losses(Zhang et al. 2021) and seriously threaten the lives and properties of the people in the mountains, the safety
39 of major projects, and restrict social and economic development (Hu et al. 2011; Hungr et al. 2005; Iverson 1997;
40 Takahashi 2014; Wu et al. 2019). Mass movements in Beijing range in scale from shallow slope failures and
41 rockfalls to catastrophic rock avalanches frequently mobilize to form debris flows, threatening the ecological
42 environment of the mountainous area (Zhong et al. 2004). Especially, in recent years, due to the superposition of
43 extreme rainstorm weather and human engineering activities, debris flow events have increased gradually(Li et al.
44 2021b). Besides, as the capital of China, Beijing has strong influence and radiation at home and abroad, where
45 geological disasters are widely concerned (Li et al. 2020a; Xie et al. 2004). With the deepening understanding of
46 debris flow disaster and the updating of database, a new and more accurate evaluation is also very necessary.
47 Therefore, it is of great significance to establishing accurate and scientific debris flow susceptibility map.

48 Through previous studies, it can be summarized that the current research on debris flow mainly focuses on the
49 following aspects: study on mechanism of debris flow, study on early warning and prediction of debris flow, study
50 on numerical simulation of debris flow and study on debris flow hazard analysis. Especially, studies on debris flow
51 hazard analysis have raised the attention of the researchers as soon as it appears(Dong et al. 2009). Communicating
52 information about debris flow hazard analysis is a crucial component of preparedness and hazard mitigation(Chiu
53 et al. 2015). Susceptibility assessment, an important part of a hazard assessment of geological processes is more
54 flexible(Li et al. 2021a). In the early days, the susceptibility assessment of debris flows was mainly qualitative
55 research. In 1976, the United Nations commissioned the International Union of Engineering Geology to conduct a
56 risk assessment of debris flows, which marked the beginning of research on the susceptibility assessment of debris
57 flows as an important research direction for disaster prevention and prediction (Li et al. 2020b). Many methods and
58 techniques (Li et al. 2020b; Wu et al. 2019) have been proposed to evaluate debris flow susceptibility assessment
59 based on different qualitative and quantitative approaches and geo-environmental information (Liu and Wang
60 1995).

61 The economy in mountainous areas is often backward, we cannot supervise and verify every basin due to the
62 limited funds. Surely, they are also wasteful and unnecessary. The debris flow susceptibility assessment can give
63 decision makers a basis for rational allocation of resources, and determine which gullies should be focused on. In
64 other words, the study plays a link role for other studies. Recently, with the development of mathematical theory,
65 computer technology, the application of 3S, the susceptibility assessment of debris flows has been extensively and
66 quantitatively studied(Li et al. 2020b). While due to the nonlinearity of debris flow system and the openness and
67 complexity of geological environment, we realize that it is chaotic, with many factors affecting the system.
68 Therefore, it is very difficult to find a unified and standard evaluation model. At present, when the information is
69 insufficient, the field investigation and experience of experts are necessary basis. However, the experience is often
70 subjective and needs a lot of professional experience accumulation. Therefore, it is very important to express the
71 experience of experts objectively and easily understandably to serve decision makers. The application of fuzzy set



72 theory in GIS environments is effective for similar problems(Luo and Dimitrakopoulos 2003; Porwal et al. 2006).
73 According to the summary above, the primary object of my present study is to explore a geographic
74 information system(GIS)-based quantitative model based on expert experience and field investigation. And the
75 model is consistent with the system characteristics of debris flow gully and can also indicate the characteristics of
76 disaster chain and that the geomorphic evolution of basin rather than simple data fitting(Porwal et al. 2006).

77 2 Study area

78 The study area is located on the northeast of Beijing, China (Fig. 1), with a total area of 948.24 square
79 kilometers. The terrain of Pinggu is high in the northeast and low in the southwest. It is surrounded by mountains,
80 account for about two-thirds of the total area, on three sides in the southeast and north. The central and southern
81 parts are alluvial plains. The area , geologically, is the West extension of the famous Jixian section, whose bedrock
82 is mainly Middle and Late Proterozoic dolomite(Lü et al. 2017) .With Pinggu District of Beijing taken as the
83 research object, the following reasons are considered: First of all, geological hazards frequently influence human
84 economic activities, so political factors must be taken into account. And within the administrative region,
85 inconsistent decision-making can be effectively avoided. Next, the regional boundary is basically divided by ridge
86 line and stream line, and the regional geological environment is relatively uniform; Last but not the least, the
87 relationship between the precision of the base map and the size of the study area is also relatively reasonable.

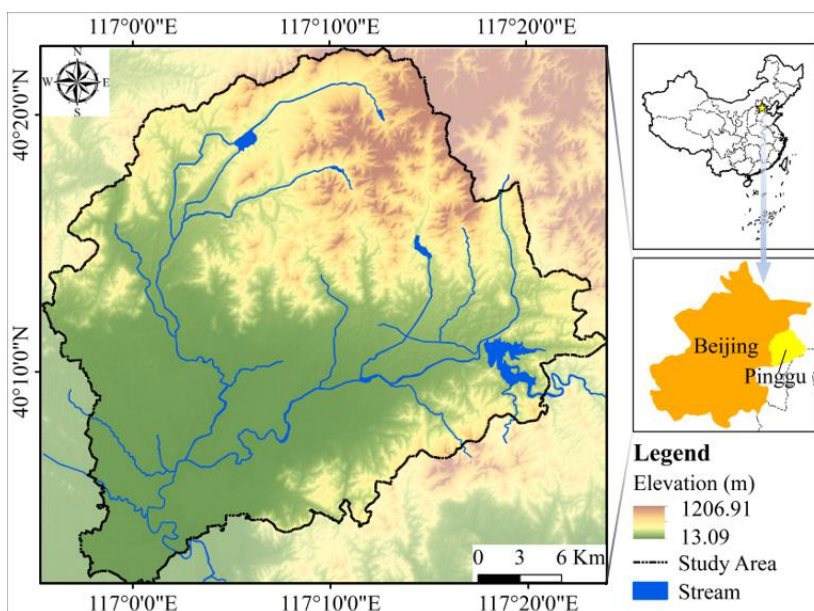


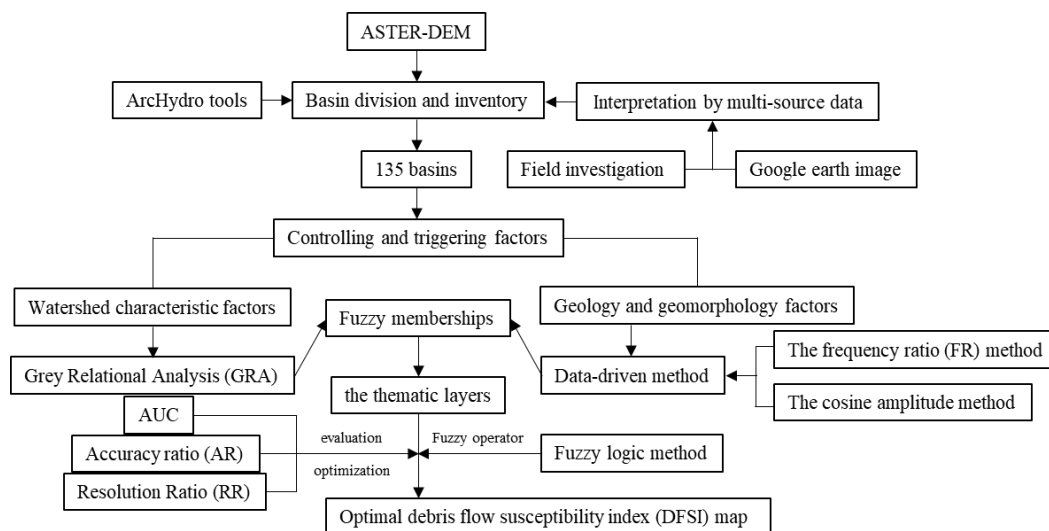
Fig. 1 Study area

90 1. Data and Methodology

91 In this study, the susceptibility assessment of debris flow hazard was based on the drainage basins unit. In a
92 debris flow susceptibility assessment model, hydro-logical response unit can fully represent the hydrological
93 process of hillside and will make the results more meaningful(Khan et al. 2013; Khan et al. 2016; Zou et al. 2019).



94 Therefore drainage networks were extracted from the ASTER-DEM by using the ArcGIS ArcHydro Toolbox and
 95 regions without obvious watershed characteristics are directly deleted. Then for each drainage basin, 19 controlling
 96 and triggering factors divided into two types were calculated. In addition, for these factors have different
 97 characteristics, different methods are used to calculate the fuzzy membership for different type factors. Because the
 98 field survey data are based on the watershed, it is scientific to make full use of qualitative understanding to
 99 determine the weight of the parameters of watershed characteristics factors; while geology and geomorphology
 100 factors are independent of watershed characteristics, it is suitable to use statistical methods to determine the
 101 objective weight. Finally, the debris flow susceptibility index (DFSI) map was derived by overlaying the factor
 102 thematic layers with fuzzy logic method. The workflow of debris flow susceptibility assessment is showed in Fig.2.
 103 Throughout the modeling process, our primary assumption here are as follows: First, while local properties surely
 104 affect the timing, size, and behavior of a mass movement, the dominant control on where they occur is the local
 105 surface topography, as it in turn defines local slope and shallow subsurface flow convergence; Second, all the
 106 evaluated basins have the possibility of debris flow; Thirdly, each evaluation factors should be available for all
 107 basins, otherwise, it should be excluded; Finally, the model should also need to integrate the system characteristics
 108 of debris flow disaster, the future development trend of climate change, and the social demand under the theoretical
 109 background of the new era to carry out reasonable modeling.



110
 111 Fig.2 Workflow of debris flow susceptibility assessment

112 **3.1 Debris flow basin division and inventory**

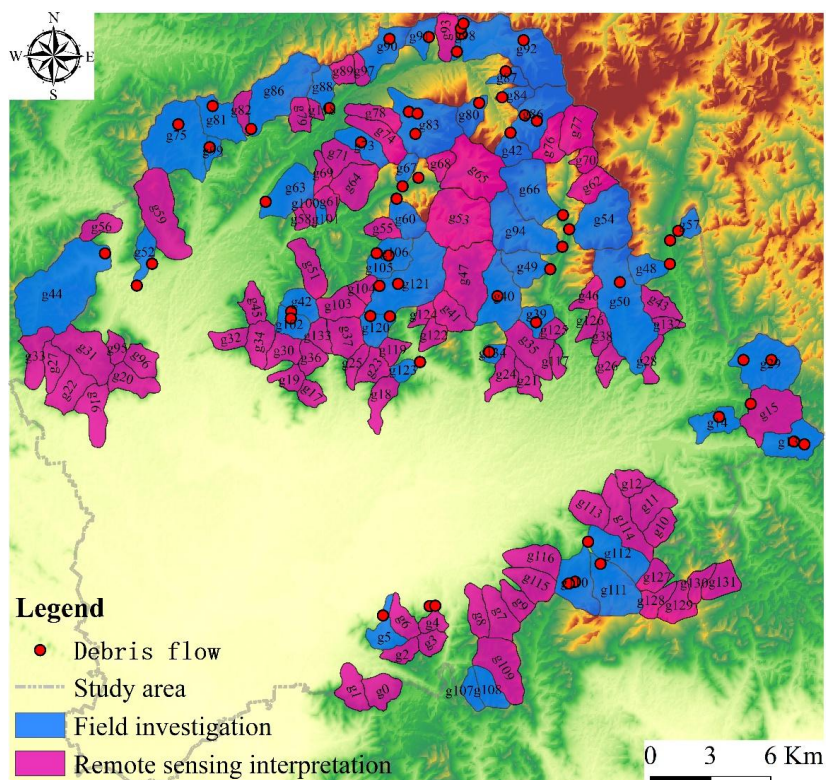
113 There are many geological hazard points in mountainous area, so it is not realistic to monitor them completely
 114 by professional team. According to the monitoring and preventing staff and the villagers, the detailed field
 115 investigation (Fig.3) for the evidence collection of debris flows will be carried out at the reported disaster point,
 116 aiming at record the loose material, delineating the basin and exploring other important information of the debris
 117 flow gullies. Moreover, field investigation is also very important for model modification. Then based on the
 118 Hydrology module in ArcGIS 10.2, the research object can be determined. Compared with grid unit and slope unit,



119 hydrological response unit for susceptibility of debris flow has greater advantages(Li et al. 2021b; Zou et al. 2019).
120 Finally, 135 basins are divided after removing the flat and irregular areas (Fig. 4), referring to the result of the field
121 investigation and the remote sensing image. In the 135 basins, 48 basins were investigated on field, accounting for
122 36%.



123
124 Fig.3 Field investigation photos. **a** Loose material; **b** Middle and Late Proterozoic dolomite; **c** colluvium deposit; **d**
125 Slope fracture; **e** Channel erosion phenomenon
126



127

128 Fig. 4 Debris flow basin division and inventory.

129 Note: The data of debris flow points comes from Beijing Municipal Commission of Planning and Natural
130 Resources

131 (http://ghzrzyw.beijing.gov.cn/zhengwuxinxi/zxzt/dzhhfztt/zhhdcpg/202008/t20200807_1976436.html)

132 3.2 Debris flow controlling and triggering factors

133 The basic requirement for the assessment of debris flows is that at least some factors included are easily
134 obtainable, are meaningful for susceptibility assessment, and can be used for evaluating the need for passive or
135 active debris flow mitigation. According to previous studies, 19 factors are selected in this paper in this study. The
136 factors are divided into two types (Table 1) because of their different characteristics. Watershed characteristic
137 factors (Type A) can be directly quantified, once the basin is determined (Fig. 5). The influence of these parameters
138 is bounded by the watershed; Geology and geomorphology factors (Type B) factors need to be further processed,
139 even if the watershed is determined. The scope of these parameters is independent of the watershed boundary.
140 Besides, rainfall and total amount of loose material source are also very important influencing factors. But
141 according to the Beijing hydrological manual, the rainfall change in the study area is not obvious, so it is not
142 considered in my model. And the total amount of loose material source cannot be obtained for the watershed
143 without on-site investigation, so calculations are impossible. In fact, we indirectly consider the influence of natural
144 loose material source by evaluating geological conditions, but cannot consider the impact of human activities.

145

146

147



148
 149

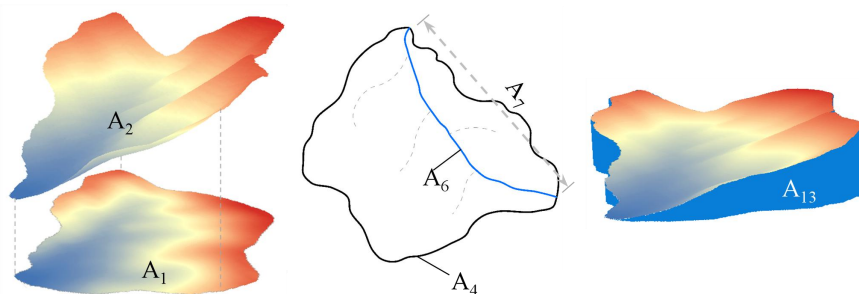
Table 1 Factors for susceptibility assessment

| Factors and Description | | Significance | obtaining ways | |
|--|-----------------|--|--|--|
| Watershed characteristic factors (Type A) | A ₁ | The planimetric (projected) area of the catchment | Geometric parameter; affecting the accumulative total volume of water and representing the potential magnitude (Cao et al. 2016; Chang and Chien 2007; Zhang et al. 2011) | derived from DEM |
| | A ₂ | The curved surface area of the catchment | Real contact area between rainfall and basin | derived from DEM |
| | A ₃ | The surface roughness of the catchment | Dimensionless parameters, reflecting the fragmentation degrees of the surface and the ground surface micro-topography. Wu et al. (2019) believe the factor can further reflects the ability of the earth to resist wind erosion. | Calculated by $A_3 = A_2 / A_1$ |
| | A ₄ | The perimeter of catchment | Geometric parameter, controlling the boundaries of a watershed | derived from DEM |
| | A ₅ | Form factor | Hydrologic parameter, related to the distribution of flow rate hydrograph (Chang and Chien 2007) | Calculated by $A_5 = \frac{A_4}{2\sqrt{\pi A_1}}$ |
| | A ₆ | The curve length of the main channel | Importance for the travel distance of materials and affecting the potential of erosive agents to dislodge and transport materials (Gómez and Kavzoglu 2005) | derived from DEM |
| | A ₇ | The straight length of the main channel | Geometric parameter, representing the change of material source in space | derived from DEM |
| | A ₈ | Bending coefficient of the main channel | Affecting the discharge situation of debris flows (Li et al. 2020b; Zhang et al. 2013) | Calculated by $A_8 = A_6 / A_7$ |
| | A ₉ | The gradient of the main channel | Hydraulic gradient parameter, affecting water transport capacity | Calculated by $A_9 = A_{12} / A_6$ |
| | A ₁₀ | Maximum elevation in the catchment | Affecting vegetation and bedrock exposure | derived from DEM |
| | A ₁₁ | Minimum elevation in the catchment | Affecting vegetation and bedrock exposure slightly | derived from DEM |
| | A ₁₂ | Maximum relative relief in the catchment | The higher the value of A ₁₂ is, the large relative relief provides favorable terrain conditions for the initiation of the debris flow source. | Calculated by $A_{12} = A_{10} - A_{11}$ |
| | A ₁₃ | Basin volume: the volume above the level of the minimum elevation in the basin | Representing the maximum material source that can be produced in an ideal state, loose material volume | derived from DEM |
| | A ₁₄ | Drainage density | Representing the geological structure, lithology, and the degree of rock weathering comprehensively and affecting the range of lateral erosions and retrogressive (Cao et al. 2016; Zhang et al. 2011) | the ratio of the total length of river network lines to A ₁ |
| Geology and geomorphology factors (Type B) | B ₁ | Lithology | Affecting the rock mass shear strength and permeability (Donati and Turrini 2002) | derived from 1:50,000 numerical geological maps |
| | B ₂ | Proximity to faults | correlated with slope failures by generally reducing the strength of the rock mass | derived from 1:50,000 |



| | | | |
|----------------|-----------------|--|---------------------------|
| | | (Dramis and Sorriso-Valvo 1994; Kellogg 2001; Korup 2004; Kritikos and Davies 2015). | numerical geological maps |
| B ₃ | Slope (degrees) | correlated with the probability of landslide occurrence (Dai and Lee 2002; He and Beighley 2008; Lee and Choi 2004). The greater the slope, the greater the vertical component of gravity (Donati and Turrini 2002), and the higher frequency of slope failures (Lee and Sambath 2006; Lee and Talib 2005) | derived from DEM |
| B ₄ | Slope aspect | affecting slope instability directly or indirectly, as a result of drying winds, sunlight, rainfall and vegetation (Dai and Lee 2002; Dai et al. 2001). | derived from DEM |
| B ₅ | Curvature | Affecting slope stability. While Lee and Talib (2005) and Ohlmacher (2007) argue on how curvature affect slope stability. | derived from DEM |

150 Note: The geological maps are provided by Beijing institute of geological and prospecting engineering and the
 151 digital elevation model-(DEM) of study area are from SRTM-DEM with a solution. of 30 m (<http://gdex.cr.usgs.gov/gdex/>).
 152
 153



154 Fig. 5 Graphical illustration of some Type A factors. A_1 is the planimetric (projected) area of the catchment; A_2 is
 155 the curved surface area of the catchment; A_4 is the perimeter of catchment; A_6 is the curve length of the main
 156 channel; A_7 is the straight length of the main channel; A_{13} is basin volume
 157

158 3.3 Fuzzy logic in susceptibility modelling

159 Fuzzy set theory proposed by Zadeh (1965) is a effective method to express the concept of partial set
 160 membership degree. This concept is different from the classical binary (two-valued) logic by using fuzzy
 161 descriptions such as low, moderate, high, steep, favourable and close to (Kritikos and Davies 2015). In the theory of
 162 fuzzy sets, elements have different degrees of membership in the interval [0,1]. 1 represents complete membership,
 163 and 0 represents non membership. Ross (1995) showed that fuzzy systems are useful in two general situations
 164 (Kritikos and Davies 2015). The method is very consistent with the characteristics of debris flow system, whose
 165 predisposing factors are fuzzy in nature and mechanism is complex and not fully understood. Application of fuzzy
 166 logic method, the most critical step is to find the suitable fuzzy membership of the factor. And fuzzy membership
 167 degree is equivalent to the weight in expert scoring method, which is calculated by objective method rather than
 168 given subjectively.



169 **3.4 fuzzy memberships**

170 **3.4.1 Grey Relational Analysis (GRA) in susceptibility modeling**

171 GRA is proposed by Deng (1982) and it is an important part of grey system theory (Wang et al. 2014).
 172 Comparing with mathematical statistics methods which need lots of sample data, typical probability distribution
 173 and large calculation, GRA is applicable to small sample size and whether the data is regular or not. There will be
 174 no inconsistency between qualitative analysis and quantitative analysis (Deng 1988). Besides it is to excogitate the
 175 leading and potential factors that affect the development of the system, and quantitatively describe the development
 176 and change trend of the system by studying whether the relative change trend of the grey factor variables with
 177 complex relationship is consistent in the process of system development and evolution (Liu et al. 2004). Thus, grey
 178 correlation analysis is introduced to quantify the correlation between each factor and the evaluation results
 179 according to field investigation expert experience. First, the procedure of GRA is to translate the performance of
 180 every alternative into a comparability sequence (Kuo et al. 2008; Lin and Lin 2002; Wei et al. 2017). Therefore,
 181 according to technical standard, “Specification of geological investigation for debris flow stabilization
 182 (DZ/T0220-2006)”, published by the China Ministry of Lands and Resources, the preliminary assessment results of
 183 debris flow susceptibility are obtained, which are used as the reference sequence of grey relation method (Table 2).
 184 Second, the grey correlation coefficient of all A factors is calculated by Eq. (1). Finally, the average grey relational
 185 coefficient (the correlation degree) is calculated by Eq. (2) as the fuzzy memberships (Table 3).

186
$$\xi_i(k) = \frac{\min_i \min_k |x_0(k) - x_i(k)| + 0.5 \max_i \max_k |x_0(k) - x_i(k)|}{|x_0(k) - x_i(k)| + 0.5 \min_i \min_k |x_0(k) - x_i(k)|} \quad (1)$$

187 Where $\xi_i(k)$ is the grey relational coefficient, $i=1, 2, \dots, n$ are the number i type A factors, $k=1, 2, \dots, n$ are the
 188 numbers of basin, $x_0(k)$ is the reference sequence (ideal target sequence), $x_i(k)$ is the number i type A factor
 189 sequence

190
$$r_i = \frac{1}{N} \sum_{k=1}^n \xi_i(k) \quad (2)$$

191 Where r_i is the correlation degree in the range (0,1). N is the total number of basins in Table 2

Table 2 Quantitative evaluation grade standard table for Debris flow susceptibility

| | | | | | | | | | | | | | |
|-------|------|------|------|------|------|------|------|------|------|------|------|------|------|
| gully | g5 | g13 | g14 | g29 | g39 | g40 | g42 | g44 | g48 | g49 | g50 | g52 | g54 |
| score | 59 | 54 | 50 | 63 | 61 | 66 | 55 | 65 | 78 | 69 | 85 | 46 | 70 |
| gully | g57 | g60 | g63 | g66 | g67 | g72 | g73 | g75 | g80 | g81 | g83 | g84 | g85 |
| score | 56 | 63 | 58 | 73 | 62 | 84 | 62 | 67 | 84 | 69 | 80 | 75 | 86 |
| gully | g86 | g87 | g88 | g90 | g91 | g92 | g94 | g98 | g99 | g101 | g102 | g105 | g106 |
| score | 73 | 84 | 60 | 70 | 80 | 84 | 71 | 78 | 61 | 65 | 67 | 65 | 70 |
| gully | g107 | g108 | g110 | g111 | g112 | g120 | g121 | g123 | g134 | - | - | - | - |
| score | 45 | 45 | 69 | 69 | 74 | 62 | 63 | 73 | 56 | - | - | - | - |

192 Note: (130≥score≥116, VH) , (115≥score≥87, M) , (86≥score≥44, L) , (43≥score≥15, N)
 193 VH=very high susceptibility, M=moderate susceptibility, L=low susceptibility, N= Non-debris flow

194
 195 Table 3 The fuzzy memberships of type A factors

| | | | | | | | |
|------------------|----------------|----------------|-----------------|-----------------|-----------------|-----------------|-----------------|
| Factor | A ₁ | A ₂ | A ₃ | A ₄ | A ₅ | A ₆ | A ₇ |
| Fuzzy membership | 0.77 | 0.77 | 0.63 | 0.6 | 0.54 | 0.55 | 0.67 |
| Factor | A ₈ | A ₉ | A ₁₀ | A ₁₁ | A ₁₂ | A ₁₃ | A ₁₄ |
| Fuzzy membership | 0.71 | 0.55 | 0.55 | 0.59 | 0.61 | 0.79 | 0.54 |



196 It can be seen from the results that the occurrence of debris flow is highly correlated with basin volume, basin area
197 and main gully bending coefficient with fuzzy membership above 0.7 in Beijing area. In the case of sufficient
198 rainfall, the basin directly determines the total amount of catchment, and the bending coefficient reflects the
199 replenishment of the source along the river. The basin volume is closely related to the number of supplementary
200 sources. Therefore, it is necessary to do well in rainfall monitoring and early warning in large watersheds, check for
201 loose matter accumulation in river basins before rainy season, and pay attention to slope protection of basin with
202 large volume potential energy for the purpose of disaster prevention and reduction.

203 3.4.2 Data-driven method in susceptibility modeling

204 Without regard to the influence of human activities, landslide is one of the main fixed sources of debris flow in
205 mountainous area. Shallow landslides are one of the most common categories of landslides. They frequently
206 involve large areas and different soils in various climatic zones (Benda and Dunne 1987; Borrelli et al. 2014; Selby
207 1982). Great debris flows may result from numerous, small slope failures that subsequently coalesce (Fairchild
208 1987; Roeloffs 1996), from flow enlargement due to incorporation of bed and bank debris (Bovis and Dagg 1992;
209 Pierson et al. 1990), or from large, individual landslides that mobilize partially or almost totally (Iverson et al. 1997;
210 Vallance and Scott 1997). Debris flows may also scour steep channels to bedrock and accelerate sediment delivery
211 to downstream, lower-gradient channels. The spatial and temporal distribution of shallow landslides are important
212 controls on landscape evolution and a major component of both natural and management-related disturbance
213 regimes in mountain drainage basins (Benda 1987; Crozier et al. 1990; Dietrich et al. 1986; Tsukamoto et al. 1982).
214 Therefore, the landslide susceptibility assessment methods can be used for reference to debris flow susceptibility
215 assessment.

216 For type B factors which cannot be characterized by a specific number, the frequency ratio (FR) method and
217 the cosine amplitude method can be used to derived their fuzzy memberships. The FR ratio defined as Eq. (3).
218 Considering the fuzzy membership must be in the interval [0,1], the FR values of the different categories are
219 normalized by the largest FR value (Lee 2006; Pradhan 2010; Pradhan 2011a; Pradhan 2011b) within the same type
220 factor (Table 4) in order to derive the function.

$$221 \quad FR = \frac{N_{(Di)}/N_{(Ci)}}{N_{(D)}/N_{(A)}} \quad (3)$$

222 where $N_{(Di)}$ is the number of debris flow pixels in the category i , $N_{(Ci)}$ is the total number of pixels in the
223 category i , $N_{(D)}$ is total number of debris flow pixels in the study area, and $N_{(A)}$ is the total number of pixels in the
224 study area.

225
226 The cosine amplitude method (Ross 1995) is widely used (Ercanoglu and Gokceoglu 2004; Ercanoglu and
227 Temiz 2011; Kanungo et al. 2009; Kanungo et al. 2006) to establish relationships among elements of two or more
228 datasets (Kritikos and Davies 2015). Assuming that n is the number of data samples (categories of a factor used in
229 the analysis) represented as an array $X = \{x_1, x_2, \dots, x_n\}$ and that each of its elements, x_i , is a vector of length m (i.e.
230 the size of the raster image) and can be expressed as $X = \{x_{11}, x_{12}, \dots, x_{im}\}$, then each element of a relation r_{ij} results
231 from a pairwise comparison of a factor category x_i with a category of the debris flow distribution layer x_j (debris
232 flow or non-debris flow). The memberships can be calculated by Eq. (4):



233

$$r_{ij} = \frac{|\sum_{k=1}^m x_{ik} x_{jk}|}{\sqrt{(\sum_{k=1}^m x_{ik}^2)(\sum_{k=1}^m x_{jk}^2)}} \quad (4)$$

234

Analogy with the study of Kanungo et al. (2006), we defined the r_{ij} value for any given factor category as the ratio of the total number of debris flow pixels in the category to the square root of the product of the total number of pixels in that category and the total number of debris flow pixels in the area. Values of r_{ij} close to 1 indicate similarity whereas values close to 0 indicate dissimilarity between the two datasets (Kritikos and Davies 2015). In order to use properly, every thematic layer must have the same pixel size.

239

240

241

242

Table 4 Factor categories and their fuzzy membership degrees

| Factor | Factor class | Number of pixels | Number of pixels classified as debris flows | Frequency ratio (FR) | Normalized frequency ratio | r_{ij} | Comprehensive ratio (FRR) |
|---------------------|---|------------------|---|----------------------|----------------------------|----------|---------------------------|
| Lithology | Quaternary sediments-unconsolidated clastic sediments | 7562017 | 48190 | 0.026 | 0.021 | 0.091 | 0.002 |
| | Coarse-grained sediments | 1148321 | 21741 | 0.076 | 0.063 | 0.061 | 0.004 |
| | Medium-grained sediments | 259619 | 12013 | 0.186 | 0.154 | 0.045 | 0.007 |
| | Fine-grained sediments | 754655 | 76380 | 0.407 | 0.337 | 0.114 | 0.038 |
| | High-grade metamorphics | 986435 | 154332 | 0.629 | 0.522 | 0.162 | 0.085 |
| | Granitoids | 725651 | 140936 | 0.781 | 0.648 | 0.155 | 0.100 |
| | Mafic extrusive | 75495 | 16398 | 0.873 | 0.724 | 0.053 | 0.038 |
| | Terrigenous clastic rock | 3289458 | 986495 | 1.205 | 1.000 | 0.41 | 0.410 |
| proximity to faults | Limestones | 8804379 | 1343754 | 0.614 | 0.509 | 0.478 | 0.243 |
| | <100 | 1057209 | 231016 | 0.878 | 1.000 | 0.198 | 0.198 |
| | 100-500 | 3778095 | 774566 | 0.824 | 0.938 | 0.363 | 0.341 |
| | 500-1000 | 3894600 | 716963 | 0.740 | 0.842 | 0.349 | 0.294 |
| | 1000-2000 | 5707265 | 760699 | 0.536 | 0.610 | 0.36 | 0.220 |
| | 2000-3000 | 2749240 | 246925 | 0.361 | 0.411 | 0.205 | 0.084 |
| slope (degrees) | >3000 | 6421103 | 69382 | 0.043 | 0.049 | 0.109 | 0.005 |
| | 0-5 | 9674508 | 153889 | 0.064 | 0.056 | 0.162 | 0.009 |
| | 5-10 | 2815606 | 383198 | 0.547 | 0.480 | 0.255 | 0.123 |
| | 10-15 | 2955913 | 521040 | 0.709 | 0.622 | 0.298 | 0.185 |
| | 15-20 | 2879704 | 570515 | 0.797 | 0.699 | 0.312 | 0.218 |
| | 20-25 | 2432724 | 498303 | 0.824 | 0.723 | 0.291 | 0.210 |
| | 25-30 | 1620325 | 350686 | 0.870 | 0.764 | 0.244 | 0.187 |
| | 30-35 | 837185 | 209574 | 1.007 | 0.883 | 0.189 | 0.167 |
| | 35-40 | 294141 | 82000 | 1.121 | 0.983 | 0.118 | 0.116 |
| | 40-45 | 77038 | 21133 | 1.103 | 0.968 | 0.06 | 0.058 |
| Slope aspect | >45 | 30091 | 8529 | 1.140 | 1.000 | 0.038 | 0.038 |
| | Flat | 380875 | 463 | 0.005 | 0.005 | 0.009 | 0.000 |
| | North | 2370048 | 296900 | 1.006 | 1.000 | 0.318 | 0.111 |
| | Northeast | 2193998 | 279917 | 0.513 | 0.510 | 0.218 | 0.092 |



| | | | | | | | |
|-----------|-------------|----------|---------|-------|-------|-------|-------|
| | East | 2873308 | 295555 | 0.414 | 0.411 | 0.224 | 0.111 |
| | Southeast | 3122267 | 353489 | 0.455 | 0.453 | 0.245 | 0.108 |
| | South | 3219111 | 354420 | 0.443 | 0.440 | 0.246 | 0.133 |
| | Southwest | 3144353 | 400064 | 0.512 | 0.509 | 0.261 | 0.135 |
| | West | 3525895 | 436381 | 0.498 | 0.495 | 0.273 | 0.140 |
| | Northwest | 2787380 | 381679 | 0.551 | 0.547 | 0.255 | 0.318 |
| Curvature | Concave | 490900 | 109157 | 0.893 | 1.000 | 0.136 | 0.136 |
| | Lessconcave | 2037602 | 394583 | 0.778 | 0.871 | 0.259 | 0.226 |
| | Flat | 18364429 | 1769210 | 0.387 | 0.433 | 0.549 | 0.238 |
| | Less convex | 2202019 | 416142 | 0.759 | 0.850 | 0.266 | 0.226 |
| | Convex | 522285 | 112740 | 0.867 | 0.971 | 0.139 | 0.135 |

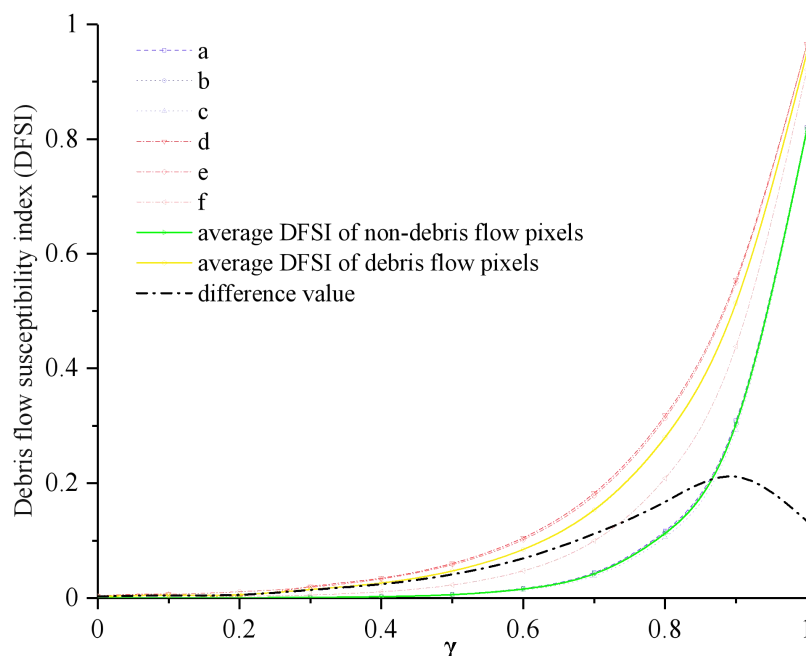
243

244 3.5 DFSI map

245 To derive the debris flow susceptibility index (DFSI) map by overlaying the factor thematic layers using fuzzy
 246 logic method, the "fuzzified" factors represented by information layers in raster format with values ranging from 0
 247 to 1 need to be combined. Compared with other four fuzzy operator, Fuzzy Gamma (Eq.6) is more suitable for the
 248 research (Kritikos and Davies 2015). To determine the appropriate γ value, the results of different gamma values
 249 were compared by the greatest distance (Kritikos and Davies 2015) between the average DFSI curves of the debris
 250 flows locations and non-debris flows locations (For example, flat pixels)(Fig. 6). Finally, 0.9 is determined for the γ
 251 value, because there is the greatest difference between debris flow and non-debris flows locations areas. In order to
 252 illustrate the superiority of our model through comparison, seventeen results are calculated in ArcGIS (Fig. 7).

$$253 \mu_{(x)} = (1 - \prod_{i=1}^n (1 - \mu_i))^\gamma * (\prod_{i=1}^n \mu_i)^{1-\gamma} \quad (5)$$

254 where $\mu_{(x)}$ is the combined membership value, μ_i is the fuzzy membership function for the i th map, $i=1,2, \dots, n$
 255 are the numbers of thematic layers to be combined, and γ is a parameter in the range (0,1).



256
257 Fig. 6 Effect of γ value on Debris flow susceptibility index (DFSIs). Curves d, e and f correspond to debris flow
258 pixels, and curves a, b and c correspond to non-debris flow area where a Debris flow is unlikely. According to
259 curve i, the maximum difference between the average DFSI values is observed for $\gamma \approx 0.9$
260

261 In order to find the optimal model, seventeen results were compared (Table 6). According to the distribution
262 map of potential geological hazard points and susceptibility map in Pinggu District published by Beijing Municipal
263 Commission of Planning and Natural Resources (BMCP&NR 2020), three indexes are used to verify the validity
264 and accuracy of the model.

265 The results of the model are independent of the model itself, so the predictive performance of the final map is
266 not just “the goodness of fit” of the data (Chung et al. 1995; Remondo et al. 2003). A relatively reliable technique
267 for quantitatively assessing how well a model is the construction of validation or success rate curves (Chung and
268 Fabbri 1999; Frattini et al. 2010; Remondo et al. 2003; Westen et al. 2003) based on a comparison between the
269 spatial distribution of debris flows and modelled debris flow susceptibility. The curves illustrate the debris flow
270 recorded in the area with respect to susceptibility values also expressed as cumulative percentages of the total area.
271 The area under the curve (AUC) defines the success rate (Marjanović et al. 2011). Generally, AUC values above 0.7
272 indicate model performance can be acceptable, while below 0.7, the performance is considered poor (Kritikos and
273 Davies 2015).

274 Although AUC is an effective evaluation method, the results is not comprehensive as mathematical features
275 for selecting the best measurement model because of insufficiency data for validation. In order to ensure the
276 objectivity of the results, we can only effectively use the recorded debris flow gully as positive, while the others as
277 negative. Thus, a two-category test is proposed to verify the model in this paper. First, the DFSI map of each model
278 are divided into two categories by Natural Breaks (Jenks) method (Fig. 7). Then the accuracy ratio (AR) is defined



279 as the frequency of the number of debris flow both classified by model and simultaneously recorded in site to the
 280 number of debris flow recorded in site. The Resolution Ratio (RR) is defined as the number of debris flow
 281 classified by model and simultaneously recorded in site to the total number debris flow classified by the model (in
 282 red color). Take R₄ for example, there are total 135 basin in the research area, but only 46 records of debris flows
 283 (Fig.3). And in the results of two categories by Natural Breaks (Jenks) method, 20 basins are divided in to debris
 284 flow, while there are only 14 debris flows among them. Then AR is calculated by dividing 14 into 46 and RR was
 285 calculated by dividing 14 into 20.

286 The higher the two values, the better the susceptibility map. Finally, the performance of models (P value) can
 287 be obtained by the Eq. (6). AUC values less than 0.6 are directly eliminated. Comparing the results of rest models,
 288 the result of R₁₆ is optimal, and the results of DFSI map are in good agreement with those of field investigation (Fig.
 289 8).

$$P = AUC + \sqrt{(AR * RR)} \quad (6)$$

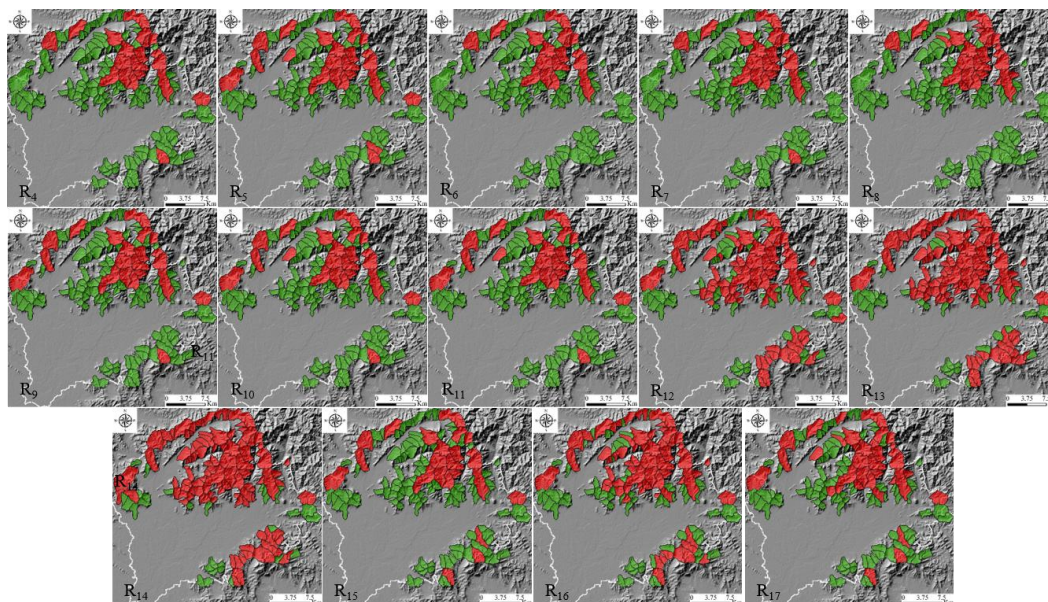
290
 291 Table 5 Predictive performance of different models

| Result and Description | | | AUC | Two-category test | | Performance index (centesimal grade) |
|---|-----------------|---|-------|---------------------|-----------------------|--------------------------------------|
| | | | | Accuracy Ratio (AR) | Resolution Ratio (RR) | |
| A factors only or B factors only | R ₁ | B factors with r _{ij} | 0.460 | / | / | / |
| | R ₂ | B factors with FR | 0.687 | / | / | / |
| | R ₃ | B factors with FRR | 0.602 | / | / | / |
| | R ₄ | All A factors | 0.786 | 0.304 | 0.700 | 83 |
| | R ₅ | Selected A factors | 0.760 | 0.391 | 0.750 | 94 |
| All factors as a single thematic layer | R ₆ | All A factors and B factors with r _{ij} | 0.776 | 0.261 | 0.667 | 74 |
| | R ₇ | All A factors and B factors with FR | 0.779 | 0.283 | 0.684 | 78 |
| | R ₈ | All A factors and B factors with FRR | 0.753 | 0.326 | 0.600 | 76 |
| | R ₉ | Selected A factors and B factors with r _{ij} | 0.746 | 0.348 | 0.727 | 86 |
| | R ₁₀ | Selected A factors B factors with FR | 0.761 | 0.348 | 0.727 | 87 |
| | R ₁₁ | Selected A factors B factors with FRR | 0.740 | 0.348 | 0.727 | 85 |
| A factors combined into one thematic layers, B factor combined into another thematic layers | R ₁₂ | All A factors and B factors with r _{ij} | 0.708 | 0.5 | 0.511 | 82 |
| | R ₁₃ | All A factors and B factors with FR | 0.753 | 0.848 | 0.394 | 99 |
| | R ₁₄ | All A factors and B factors with FRR | 0.711 | 0.870 | 0.404 | 96 |
| | R ₁₅ | Selected A factors and B factors with r _{ij} | 0.726 | 0.348 | 0.667 | 80 |
| | R ₁₆ | Selected A factors and B factors with FR | 0.768 | 0.739 | 0.442 | 100 |
| | R ₁₇ | Selected A factors B factors with FRR | 0.740 | 0.457 | 0.600 | 88 |

292 Note: Selected A factors with fuzzy membership more than 0.6; FRR represents the product of FR and r_{ij};
 293 Performance index is normalized by the largest FR value



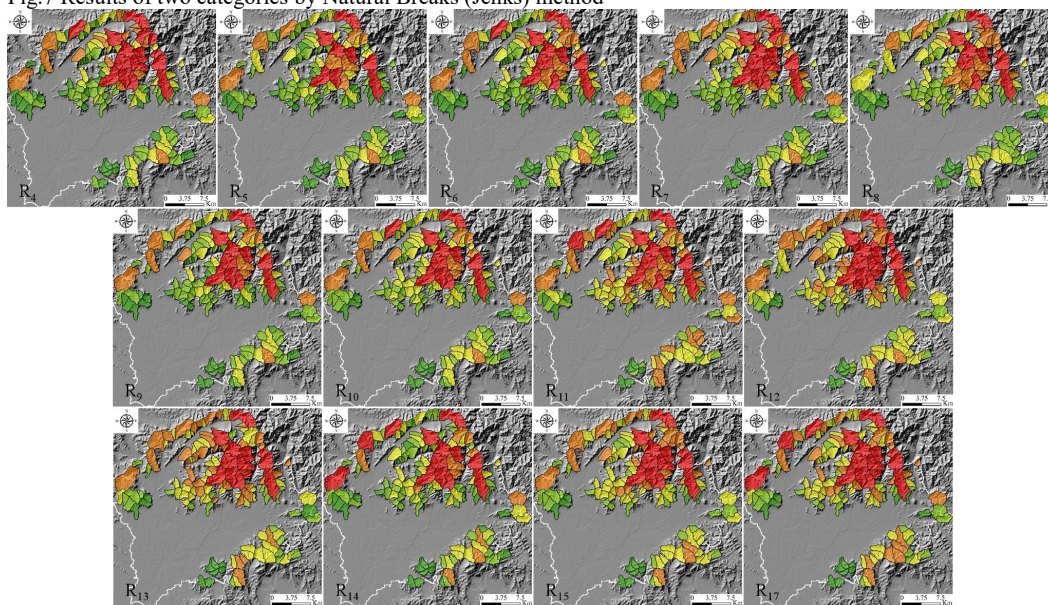
294



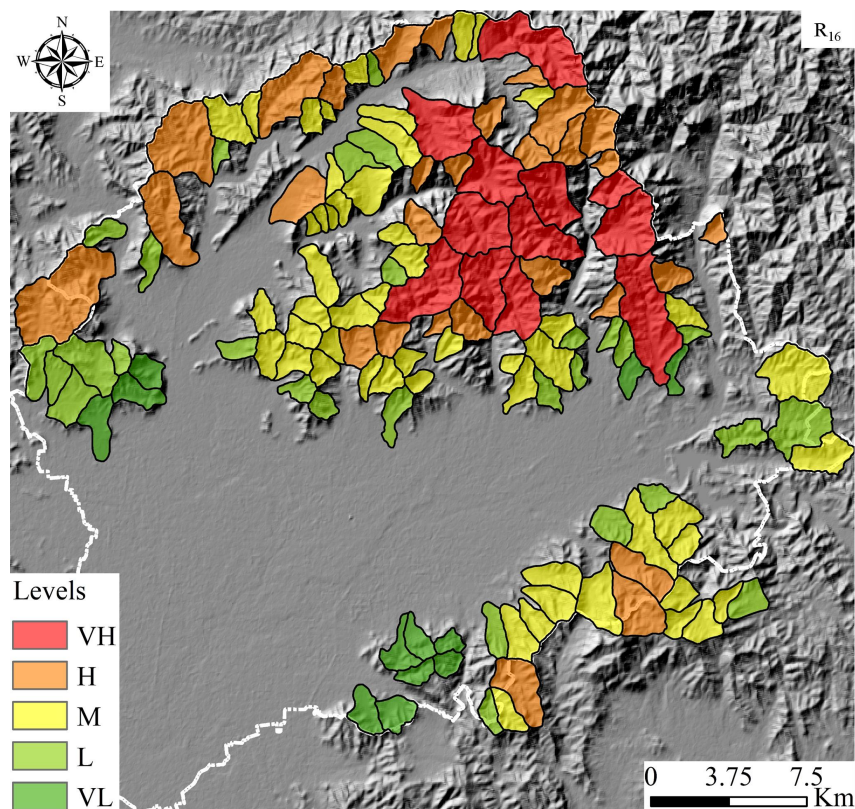
295

296

Fig.7 Results of two categories by Natural Breaks (Jenks) method



297



298
299 Fig 8 Debris flow susceptibility maps

300 4 Results and Discussion

301 According to the previous researches, 19 factors are selected. Although these factors cannot fully evaluate the
302 character of a basin, it is necessary to consider that they are easily obtainable for each basin and can be obtained
303 relatively accurately, ensuring that the model can be widely applied. Vegetation and rainfall factors are also very
304 important, but there is little difference in vegetation and rainfall across the study area. Considering the background
305 of global climate change, high temperature and extreme rainfall events will be increasing, which also makes them
306 uncertain factor compared with factors compared. As for the factors describing debris flow magnitude, usually,
307 several channels have the recorded data. Other factors that also influence the susceptibility of debris flow are
308 usually difficult to obtain, including soil drainage, induration, thickness, conductivity, and strength properties;
309 subsurface flow orientation; bedrock fracture flow; and root strength.

310 The predictive performance of the output debris flow susceptibility maps, obtained from seventeen different
311 models, is verified by comparing with maps published by authority. By comparing the results, the following results
312 are discussed:

313 First, comparing R_1 , R_2 , R_3 , R_4 and R_5 , it can be concluded that the model based on field investigation and
314 expert experience is more effective than data-driven directly, when the sufficient information cannot be obtained.
315 This is mainly because when the basin area reaches a certain size, it is no longer controlled by one or several



316 factors, but becomes a complex system. It is not only the factors that affect the system, but also the system will
317 react on each factor. Geomorphic evolution is basically the result of the interaction of the endogenic and exogenic
318 geological processes. A geological period can be regarded as the beginning of an endogenic geological processes to
319 the next one. In the early stage of geological period, endogenic geological processes play a major role, and in the
320 later relatively stable period, exogenic geological processes will play a more and more important role. In this large
321 cycle, the basin continuously occurs a small cycle of accumulating and releasing energy, which leads to extremely
322 complex system changes. In addition, there is a contradiction between the scale of geological evolution and the
323 scale of engineering activities. So limited information can be obtained under these conditions that leads to the
324 unreliability of data-driven evaluation. Therefore, in the current period, field investigation and expert experience
325 are fundamental.

326 Second, by comparing R_4 and R_5 , R_6 and R_9 , R_7 and R_{10} , R_8 and R_{11} , R_{12} and R_{15} , R_{13} and R_{16} , R_{14} and R_{17} , it
327 can be concluded that the accuracy and resolution of the model can be improved by simplifying the factors, which
328 will eliminate the weak correlation and independence factors. In practical application, even if the susceptibility map
329 is obtained, the classification of the susceptibility degree is still a very difficult problem. Because everyone's
330 subjective definition of "susceptibility degree" is different. By simplifying the factors, the main factors can be
331 selected, which magnifies the differences between basins, so the boundaries between different susceptibility
332 degrees are more obvious.

333 Third, by comparing R_6 and R_{12} , R_7 and R_{13} , R_8 and R_{14} , R_9 and R_{15} , R_{10} and R_{16} , R_{11} and R_{17} , it can be
334 concluded that the model in which factors are classified into two types is better than the method in which all factors
335 as a single thematic layer without classification. Because the factors categorized separately are more closely linked
336 and has consistent influence on the system in mechanism. We can also infer that the non-linear combination
337 characteristics between different types are stronger and scientific classification can improve the performance of the
338 model.

339 Fourth, comparing R_{12} and R_{13} , R_{15} and R_{16} , it can be concluded that the frequency ratio method is better than
340 the cosine amplitude method in the study. Different from the study of Kritikos et al. (2015), the watershed unit
341 rather than the grid unit is used, which indicates that the former has a wide range of application, while the latter has
342 a disadvantage of strict conditions.

343 Based on the results of the above four analyses, the most optimal model should have the features of being
344 based on expert experience, using selected factors, classifying factors before using them, and using frequency ratio
345 method. Then the model R_{16} is selected according to the features, which is well in accordance with theoretical
346 method performance score, and gets fine mutual verification.

347 In summary, the debris flow susceptibility assessment in this study follows the principles of scientific and
348 practicality. First, classification of influencing factors follows the principles of scientific, which require the
349 classification to be accurate and systematic. Then the same susceptibility degree can be classified into the same
350 type reasonably. In order to correctly classify the factors, it is necessary to grasp the characteristics of the formation,
351 movement and accumulation of debris flow. Therefore, the classification should comprehensively consider the
352 development background (geology, geomorphology, climate, hydrology, soil, vegetation, human activities and other
353 factors). The practical principle refers to that the study should not only fully obtain scientific and accurate results,



354 but also make the professional results understood by decision makers. The relative simplicity of the model with
355 data easy to obtain is attractive, which can also provide necessary information for debris flow mitigation and land
356 utilization. Although the susceptibility grade and susceptibility value of each watershed is obtained, the results are
357 relatively effective in this study area. The purpose is to distinguish the difference of each channel for
358 decision-making to work out pertinence measure. Once separated from this study area, the comparison with other
359 regions in value will lose its practical significance. In addition, with the development of technology and theory, we
360 should replace some traditional factors which are not easy to quantify with more precise quantitative factors to
361 improve the efficiency and accuracy of evaluation, such as surface roughness instead of drainage density. Last,
362 nonlinear methods is consistent with the nonlinear characteristics of debris flow system.

363 **5 Conclusion**

364 In the present study, a new combination model for debris-flow susceptibility based on GIS was developed in
365 Pinggu, the eastern of Beijing. The objective and motivation of this study is to demonstrate a simple, extensible,
366 and convenient analytical model for the debris flow prediction. Three methods are selected in the model with their
367 own advantages. GRA has great advantages in the case of less samples, data-driven method is mainly used to
368 reduce subjectivity and fuzzy logic is fitted to solve nonlinear problems with fuzzy classification. The output debris
369 flow susceptibility maps obtained from the optimal models demonstrated satisfactory performance predicting
370 approximately 50 % of the debris flow gully with the relative higher susceptibility values corresponding to
371 $AUC \geq 0.7$. Considering that the data used for verification is only the recorded debris flow points rather than all
372 debris flow records in the area, its accuracy should be higher. The predictive performance of the susceptibility maps
373 and the spatial correlation of debris flow gully with H and VH susceptibility with recorded debris flow illustrate
374 that the assessment at regional scale using the proposed method is feasible. Compared with the previous results
375 based on grid units in this area, the evaluation results are basically the same, but they are more targeted for debris
376 flow disasters for decision makers {Li, 2020 #278}. Besides, considering that the meaning of the used factors is
377 clear and the data easy to obtain, these conditions mentioned enable the model to be widely applied.

378 Preliminary research indicates that: First of all, the relatively ideal evaluation results are obtained by
379 combining the landslide susceptibility analysis method with the debris flow. It reveals a systematic idea and disaster
380 chain phenomenon. Further more, we should pay more attention to the relative susceptibility value rather than
381 absolute values in different models, unless we need further study such as risk assessment. It is realized that the
382 performance of the model is, to a great extent, determined by the effect of its classification. What's more,
383 comprehensive consideration of endogenic and exogenic geological processes in susceptibility assessment has
384 better expected results. Last but not least, under the engineering geological environment with acceptable difference,
385 it has advantages of practical significance to regard the administrative region as a research area for policy making.
386 because different regions have different status constraints in population quality and economy. In short, an effort has
387 been made to develop a cost- and time-efficient debris flow susceptibility assessment with an acceptable degree of
388 accuracy for regional-scale planning and contribute to making hazard, susceptibility and risk maps more accessible
389 to individuals and local authorities. The evolution of GIS-based methods and modern data availability especially
390 through online databases significantly contribute towards this aim. However, a challenge remains in producing



391 results with meaningful accuracy for the scale of planning, using available resources. Previous studies, as well as
392 the present work, highlight that the effectiveness of the final map depends on the quality of input data. Comparison
393 with a very high-resolution LIDAR-derived DEM indicated that the spatial accuracy of the DEM varies between
394 different landforms (lakes, river channels, riverbeds, floodplains etc.) and the areas of greatest errors are
395 predominantly confined to valley floors .However, with overall RMS error of 8.15 m, the DEM meets the
396 internationally accepted accuracy standards as set out by US Geological Survey (USGS 1997) and is of sufficient
397 quality for regional-scale studies such as the present one. Updating and improving existing debris flow catalogues
398 and inventories are crucial for the development of reliable susceptibility and risk assessment methods.

399 **Acknowledgements**

400 This research was financially supported by the Key Project of NSFC-Yunnan Joint Fund (Grant no. U1702241) and
401 the National Key Research and Development Plan (Grant No. 2018YFC1505301). The authors would like to thank
402 Yuchao Li, Zhihai Li, Jiejie Shen, Feifan Gu et al. for their contributions to the collection of field data, and the editor and
403 anonymous reviewers for their comments and suggestions which helped a lot in making this paper better.
404



405 **Reference**

- 406 Benda LE (1987) Sediment routing by debris flow
- 407 Benda LE, Dunne T (1987) Sediment routing by debris flow. In: Beschta RL, Blinn T, Grant GE, Swanson FJ, Ice GG (eds) Erosion
408 and sedimentation in the Pacific Rim, vol 165. IAHS Publ, pp 213-223. doi:doi:10.1111/j.1753-4887.1977.tb06503.x
- 409 BMCP&NR (2020) The distribution map of potential geological hazard points and susceptibility map in pinggu district.
410 http://ghzrzyw.beijing.gov.cn/zhengwuxinxi/zxzt/dzwhfztt/zzzhdcpj/202008/t20200807_1976436.html.
- 411 Borrelli L, Cofone G, Coscarelli R, Gullà G (2014) Shallow landslides triggered by consecutive rainfall events at Catanzaro strait
412 (Calabria–Southern Italy) Journal of Maps 11:730-744 doi:10.1080/17445647.2014.943814
- 413 Bovis M, Dagg B (1992) Debris flow triggering by impulsive loading - mechanical modeling and case-studies Canadian Geotechnical
414 Journal 29:345-352 doi:10.1139/t92-040
- 415 Cao C, Xu P, Chen J, Zheng L, Niu C (2016) Hazard assessment of debris-flow along the baicha river in heshigten banner, inner
416 mongolia, china Int J Environ Res Public Health 14:1-19 doi:10.3390/ijerph14010030
- 417 Chang TC, Chien YH (2007) The application of genetic algorithm in debris flows prediction Environmental Geology 53:339-347
418 doi:10.1007/s00254-007-0649-2
- 419 Chiou IJ, Chen CH, Liu WL, Huang SM, Chang YM (2015) Methodology of disaster risk assessment for debris flows in a river basin
420 Stoch Env Res Risk A 29:775-792 doi:10.1007/s00477-014-0932-1
- 421 Chung C-JF, Fabbri AG (1999) Probabilistic prediction models for landslide hazard mapping Photogrammetric Engineering And
422 Remote Sensing 65:1389-1399 doi:10.1016/S0924-2716(99)00030-1
- 423 Chung C-JF, Fabbri A, Westen CJv (1995) Multivariate regression analysis for landslide hazard zonation Geographical Information
424 Systems in Assessing Natural Hazards 5:107-133
- 425 Crozier MJ, Vaughan EE, Tippett JM (1990) Relative instability of colluvium-filled bedrock depressions Earth Surface Processes and
426 Landforms 15:329-339 doi:10.1002/esp.3290150404
- 427 Dai FC, Lee CF (2002) Landslide characteristics and slope instability modeling using GIS, Lantau Island, Hong Kong Geomorphology
428 42:213-228 doi:10.1016/S0169-555X(01)00087-3
- 429 Dai FC, Lee CF, Li H-Z, Xu C (2001) Assessment of landslide susceptibility on the natural terrain of Lantau Island, Hong Kong
430 Environmental Geology 40:381-391 doi:10.1007/s002540000163
- 431 Deng JL (1982) Control problems of grey systems Systems and Control Letters 1:288-294 doi:10.1016/S0167-6911(82)80025-X
- 432 Deng JL (1988) Grey prediction and decision. Huazhong University of Science and Technology Press, Wuhan
- 433 Di B et al. (2019) Assessing susceptibility of debris flow in southwest china using gradient boosting machine Sci Rep 9:12532
434 doi:10.1038/s41598-019-48986-5
- 435 Dietrich WE, Wilson CJ, Reneau SL (1986) Hollows, colluvium, and landslides in soil-mantled landscapes. In: Abrahams. AD (ed)
436 Hillslope Processes. Allen & Unwin, Boston,
- 437 Donati L, Turrini MC (2002) An objective method to rank the importance of the factors predisposing to landslides with the GIS
438 methodology: application to an area of the Apennines (Valnerina; Perugia, Italy) Engineering Geology 63:277-289
439 doi:10.1016/S0013-7952(01)00087-4
- 440 Dong J-J, Lee C-T, Tung Y-H, Liu C-N, Lin K-P, Lee J-F (2009) The role of the sediment budget in understanding debris flow
441 susceptibility Earth Surface Processes and Landforms 34:1612-1624 doi:10.1002/esp.1850
- 442 Dramis F, Sorriso-Valvo M (1994) Deep-seated gravitational slope deformations, related landslides and tectonics Engineering Geology
443 38:231-243 doi:10.1016/0013-7952(94)90040-X
- 444 Ercanoglu M, Gokceoglu C (2004) Use of fuzzy relations to produce landslide susceptibility map of a landslide prone area (West
445 Black Sea Region, Turkey) Engineering Geology 75:229-250 doi:10.1016/j.enggeo.2004.06.001
- 446 Ercanoglu M, Temiz FA (2011) Application of logistic regression and fuzzy operators to landslide susceptibility assessment in Aздavay
447 (Kastamonu, Turkey) Environmental Earth Sciences 64:949-964 doi:10.1007/s12665-011-0912-4
- 448 Fairchild LH (1987) The importance of lahar initiation processes Reviews in Engineering Geology 7:51-62 doi:10.1130/REG7-p51



- 449 Frattini P, Crosta G, Carrara A (2010) Techniques for evaluating the performance of landslide susceptibility models *Engineering*
450 *Geology* 111:62-72 doi:10.1016/j.enggeo.2009.12.004
- 451 Gómez H, Kavzoglu T (2005) Assessment of shallow landslide susceptibility using artificial neural networks in Jabonosa River Basin,
452 Venezuela *Engineering Geology* 78:11-27 doi:10.1016/j.enggeo.2004.10.004
- 453 He Y, Beighley RE (2008) GIS-based regional landslide susceptibility mapping: a case study in southern California *Earth Surface*
454 *Processes and Landforms* 33:380-393 doi:10.1002/esp.1562
- 455 Hu K, Wei F, Li Y (2011) Real-time measurement and preliminary analysis of debris-flow impact force at Jiangjia Ravine, China *Earth*
456 *Surface Processes and Landforms* 36:1268-1278 doi:10.1002/esp.2155
- 457 Hungr O, McDougall S, Bovis M (2005) Entrainment of material by debris flows. In: Jakob M, Hungr O (eds) *Debris-flow Hazards*
458 *and Related Phenomena*. Praxis.Springer Berlin Heidelberg, pp 135-158
- 459 Iverson RM (1997) The physics of debris flows *Reviews of Geophysics* 35:245-296. doi:10.1029/97RG00426
- 460 Iverson RM, Reid ME, LaHusen RG (1997) Debris-flow mobilization from landslides *Annual Review of Earth and Planetary Sciences*
461 25:85-138 doi:10.1146/annurev.earth.25.1.85
- 462 Kanungo DP, Arora M, Sarkar S, Gupta R (2009) A fuzzy set based approach for integration of thematic maps for landslide
463 susceptibility zonation *Georisk* 3 doi:10.1080/17499510802541417
- 464 Kanungo DP, Arora MK, Sarkar S, Gupta RP (2006) A comparative study of conventional, ANN black box, fuzzy and combined neural
465 and fuzzy weighting procedures for landslide susceptibility zonation in Darjeeling Himalayas *Engineering Geology*
466 85:347-366 doi:10.1016/j.enggeo.2006.03.004
- 467 Kellogg KS (2001) Tectonic controls on a large landslide complex: Williams Fork Mountains near Dillon, Colorado *Geomorphology*
468 41:355-368 doi:10.1016/S0169-555X(01)00067-8
- 469 Khan U, Tuteja NK, Sharma A (2013) Delineating hydrologic response units in large upland catchments and its evaluation using soil
470 moisture simulations *Environmental Modelling & Software* 46:142-154 doi:10.1016/j.envsoft.2013.03.005
- 471 Khan U, Tuteja NK, Sharma A, Lucas S, Murphy B, Jenkins B (2016) Applicability of Hydrologic Response Units in low topographic
472 relief catchments and evaluation using high resolution aerial photograph analysis *Environmental Modelling & Software*
473 81:56-71 doi:10.1016/j.envsoft.2016.03.010
- 474 Korup O (2004) Geomorphic implications of fault zone weakening Slope instability along the Alpine Fault South Westland to
475 Fiordland New Zealand *Journal of Geology and Geophysics* 47:257-267 doi:10.1080/00288306.2004.9515052
- 476 Kritikos T, Davies T (2015) Assessment of rainfall-generated shallow landslide/debris-flow susceptibility and runoff using a
477 GIS-based approach: application to western Southern Alps of New Zealand *Landslides* 12:1051-1075
478 doi:10.1007/s10346-014-0533-6
- 479 Kuo Y, Yang T, Huang G-W (2008) The use of grey relational analysis in solving multiple attribute decision-making problems
480 *Computers & Industrial Engineering* 55:80-93 doi:10.1016/j.cie.2007.12.002
- 481 Lee S (2006) Application and verification of fuzzy algebraic operators to landslide susceptibility mapping *Environmental Geology*
482 52:615-623 doi:10.1007/s00254-006-0491-y
- 483 Lee S, Choi J (2004) Landslide susceptibility mapping using GIS and the weight-of-evidence model *International Journal of*
484 *Geographical Information Science* 18:789-814 doi:10.1080/13658810410001702003
- 485 Lee S, Sambath T (2006) Landslide susceptibility mapping in the Damrei Romel area, Cambodia using frequency ratio and logistic
486 regression models *Environmental Geology* 50:847-855 doi:10.1007/s00254-006-0256-7
- 487 Lee S, Talib JA (2005) Probabilistic landslide susceptibility and factor effect analysis *Environmental Geology* 47:982-990
488 doi:10.1007/s00254-005-1228-z
- 489 Li Y, Chen J, Li Z, Han X, Zhai S, Li Y, Zhang Y (2021a) A case study of debris flow risk assessment and hazard range prediction
490 based on a neural network algorithm and finite volume shallow water flow model *Environmental Earth Sciences* 80
491 doi:10.1007/s12665-021-09580-z
- 492 Li Y, Chen J, Tan C, Li Y, Gu F, Zhang Y, Mehmood Q (2020a) Application of the borderline-SMOTE method in susceptibility



- 493 assessments of debris flows in Pinggu District, Beijing, China *Natural Hazards* 105:2499-2522
494 doi:10.1007/s11069-020-04409-7
- 495 Li Y, Chen J, Zhang Y, Song S, Han X, Ammar M (2020b) Debris flow susceptibility assessment and runout prediction: A case study in
496 shiyang gully, beijing, china *International Journal of Environmental Research* 14:365-383 doi:10.1007/s41742-020-00263-4
- 497 Li Z, Chen J, Tan C, Zhou X, Li Y, Han M (2021b) Debris flow susceptibility assessment based on topo-hydrological factors at
498 different unit scales: a case study of Mentougou district, Beijing *Environmental Earth Sciences* 80
499 doi:10.1007/s12665-021-09665-9
- 500 Lin CL, Lin CL (2002) The use of the orthogonal array with grey relational analysis to optimize the electrical discharge machining
501 process with multiple performance characteristics *International Journal of Machine Tools and Manufacture* 42:237-244
502 doi:10.1016/S0890-6955(01)00107-9
- 503 Liu L, Wang S (1995) Fuzzy comprehensive evaluation on landslide and debris flow risk degree in Zaotong, Yunnan Mountain
504 Research 13:261-266
- 505 Liu S, Dang Y, Fang Z (2004) Grey system theory and its applications. Science Press, Beijing
- 506 Lü J, Wang C, Liu H, Zhang X (2017) Division of beijing geological environment system *Urban geology* 12:19-25
507 doi:10.3969/j.issn.1007-1903.2017.03.004
- 508 Luo X, Dimitrakopoulos R (2003) Data-driven fuzzy analysis in quantitative mineral resource assessment *Computers & Geosciences*
509 29:3-13 doi:10.1016/s0098-3004(02)00078-x
- 510 Marjanović M, Kovačević M, Bajat B, Voženilek V (2011) Landslide susceptibility assessment using SVM machine learning algorithm
511 *Engineering Geology* 123:225-234 doi:10.1016/j.enggeo.2011.09.006
- 512 Ohlmacher GC (2007) Plan curvature and landslide probability in regions dominated by earth flows and earth slides *Engineering*
513 *Geology* 91:117-134 doi:10.1016/j.enggeo.2007.01.005
- 514 Pierson TC, Janda RJ, Thouret J-C, Borrero CA (1990) Perturbation and melting of snow and ice by the 13 November 1985 eruption of
515 Nevado del Ruiz, Colombia, and consequent mobilization, flow and deposition of lahars *Journal of Volcanology and*
516 *Geothermal Research* 41:17-66 doi:10.1016/0377-0273(90)90082-q
- 517 Porwal A, Carranza EJM, Hale M (2006) A Hybrid Fuzzy Weights-of-Evidence Model for Mineral Potential Mapping *Natural*
518 *Resources Research* 15:1-14 doi:10.1007/s11053-006-9012-7
- 519 Pradhan B (2010) Landslide susceptibility mapping of a catchment area using frequency ratio, fuzzy logic and multivariate logistic
520 regression approaches *Journal of the Indian Society of Remote Sensing* 38:301-320 doi:10.1007/s12524-010-0020-z
- 521 Pradhan B (2011a) Manifestation of an advanced fuzzy logic model coupled with Geo-information techniques to landslide
522 susceptibility mapping and their comparison with logistic regression modelling *Environmental and Ecological Statistics*
523 18:471-493 doi:10.1007/s10651-010-0147-7
- 524 Pradhan B (2011b) Use of GIS-based fuzzy logic relations and its cross application to produce landslide susceptibility maps in three
525 test areas in Malaysia *Environmental Earth Sciences* 63:329-349 doi:10.1007/s12665-010-0705-1
- 526 Remondo J, González A, Terán JRDD, Cendrero A, Fabbri A, Chung C-JF (2003) Validation of landslide susceptibility maps;
527 examples and applications from a case study in northern Spain *Natural Hazards* 30:437-449
528 doi:10.1023/B:NHAZ.0000007201.80743.fc
- 529 Roeloffs E (1996) Poroelastic techniques in the study of earthquake-related hydrologic phenomena 38:135-195
530 doi:10.1016/S0065-2687(08)60270-8
- 531 Ross TJ (1995) Fuzzy logic with engineering applications. McGraw-Hill, New York
- 532 Selby MJ (1982) Hillslope materials and processes. Oxford University Press, Oxford
- 533 Takahashi T (2014) Debris flow mechanics, prediction and countermeasures. second edn. Taylor & Francis/Balkema, The Netherlands
- 534 Tsukamoto Y, Ohta T, Noguchi H (1982) Hydrological and geomorphological studies of debris slides on forested hillslopes in Japan
535 *Journal des Sciences Hydrologiques* 27:234
- 536 Vallance JW, Scott KM (1997) The Osceola mudflow from Mount Rainier: Sedimentology and hazard implications of a huge clay-rich



- 537 debris flow Geological Society of America Bulletin 109:143-163
538 doi:10.1130/0016-7606(1997)109<0143:TOMFMR>2.3.CO;2
- 539 Wang J, Yu Y, Yang S, Lu G-h, Ou G-q (2014) A modified certainty coefficient method (M-CF) for debris flow susceptibility
540 assessment: A case study for the Wenchuan earthquake meizoseismal areas Journal of Mountain Science 11:1286-1297
541 doi:10.1007/s11629-013-2781-7
- 542 Wei Z, Shang Y, Zhao Y, Pan P, Jiang Y (2017) Rainfall threshold for initiation of channelized debris flows in a small catchment based
543 on in-site measurement Engineering Geology 217:23-34 doi:10.1016/j.enggeo.2016.12.003
- 544 Westen CJv, Rengers N, Soeters R (2003) Use of geomorphological information in indirect landslide susceptibility assessment Natural
545 Hazards 30:399-419 doi:10.1023/B:NHAZ.0000007097.42735.9e
- 546 Wu S, Chen J, Zhou W, Iqbal J, Yao L (2019) A modified Logit model for assessment and validation of debris-flow susceptibility
547 Bulletin of Engineering Geology and the Environment 78:4421-4438 doi:10.1007/s10064-018-1412-5
- 548 Xie H, Zhong D, Wei F, Wang S (2004) Classification of debris flow in the mountains of Beijing Journal of mountain science
549 22:212-219 doi:10.16089/j.cnki.1008-2786.2004.02.013
- 550 Zadeh LA (1965) Fuzzy sets Information & Control 8:338-353 doi:10.1016/S0019-9958(65)90241-X
- 551 Zhang W, Chen J-p, Wang Q, An Y, Qian X, Xiang L, He L (2013) Susceptibility analysis of large-scale debris flows based on
552 combination weighting and extension methods Natural Hazards 66:1073-1100 doi:10.1007/s11069-012-0539-0
- 553 Zhang W, Li HZ, Chen Jp, Zhang C, Xu Lm, Sang Wf (2011) Comprehensive hazard assessment and protection of debris flows along
554 Jinsha River close to the Wudongde dam site in China Natural Hazards 58:459-477 doi:10.1007/s11069-010-9680-9
- 555 Zhang Y, Chen J, Tan C, Bao Y, Han X, Yan J, Mehmood Q (2021) A novel approach to simulating debris flow runout via a
556 three-dimensional CFD code: a case study of Xiaojia Gully Bulletin of Engineering Geology and the Environment
557 80:5293-5313 doi:10.1007/s10064-021-02270-x
- 558 Zhong D, Xie H, Wang S, Wei F, Jin H (2004) Debris flow in Beijing mountain. Commercial Press, Beijing
- 559 Zou Q, Cui P, He J, Lei Y, Li S (2019) Regional risk assessment of debris flows in China—An HRU-based approach Geomorphology
560 340:84-102 doi:10.1016/j.geomorph.2019.04.027
561